Correlative nm-Scale Nonuniformity of Active Charge Carriers and Electrical Potential along both the Plane-View and Depth Directions in Group-V-Doped CdTe Thin Films

Preprint

Chun-Sheng Jiang, John Moseley, Chunxioao Xiao, Wyatt Metzger, and Mowafak Al-Jassim

National Renewable Energy Laboratory

Presented at the 47th IEEE Photovoltaic Specialists Conference (PVSC 47)
June 15 – August 21, 2020

NREL is a national laboratory of the U.S. Department of Energy
Office of Energy Efficiency & Renewable Energy
Operated by the Alliance for Sustainable Energy, LLC

Conference Paper
NREL/CP-5K00-76040
August 2020

This report is available at no cost from the National Renewable Energy Laboratory (NREL) at www.nrel.gov/publications.

Contract No. DE-AC36-08GO28308

Correlative nm-Scale Nonuniformity of Active Charge Carriers and Electrical Potential along both the Plane-View and Depth Directions in Group-V-Doped CdTe Thin Films

Preprint

Chun-Sheng Jiang, John Moseley, Chunxioao Xiao, Wyatt Metzger, and Mowafak Al-Jassim

National Renewable Energy Laboratory

Suggested Citation
Jiang, Chun-Sheng, John Moseley, Chunxioao Xiao, Wyatt Metzger, and Mowafak Al-Jassim. 2020. *Correlative nm-Scale Nonuniformity of Active Charge Carriers and Electrical Potential along both the Plane-View and Depth Directions in Group-V-Doped CdTe Thin Films: Preprint*. Golden, CO: National Renewable Energy Laboratory. NREL/CP-5K00-76040. https://www.nrel.gov/docs/fy20osti/76040.pdf.

© 2020 IEEE. Personal use of this material is permitted. Permission from IEEE must be obtained for all other uses, in any current or future media, including reprinting/republishing this material for advertising or promotional purposes, creating new collective works, for resale or redistribution to servers or lists, or reuse of any copyrighted component of this work in other works.

NREL is a national laboratory of the U.S. Department of Energy
Office of Energy Efficiency & Renewable Energy
Operated by the Alliance for Sustainable Energy, LLC

This report is available at no cost from the National Renewable Energy Laboratory (NREL) at www.nrel.gov/publications.

Contract No. DE-AC36-08GO28308

Conference Paper
NREL/CP-5K00-76040
August 2020

National Renewable Energy Laboratory
15013 Denver West Parkway
Golden, CO 80401
303-275-3000 • www.nrel.gov

NOTICE

This work was authored in part by the National Renewable Energy Laboratory, operated by Alliance for Sustainable Energy, LLC, for the U.S. Department of Energy (DOE) under Contract No. DE-AC36-08GO28308. Funding provided by U.S. Department of Energy Office of Energy Efficiency and Renewable Energy Solar Energy Technologies Office. The views expressed herein do not necessarily represent the views of the DOE or the U.S. Government. The U.S. Government retains and the publisher, by accepting the article for publication, acknowledges that the U.S. Government retains a nonexclusive, paid-up, irrevocable, worldwide license to publish or reproduce the published form of this work, or allow others to do so, for U.S. Government purposes.

This report is available at no cost from the National Renewable Energy Laboratory (NREL) at www.nrel.gov/publications.

U.S. Department of Energy (DOE) reports produced after 1991 and a growing number of pre-1991 documents are available free via www.OSTI.gov.

Cover Photos by Dennis Schroeder: (clockwise, left to right) NREL 51934, NREL 45897, NREL 42160, NREL 45891, NREL 48097, NREL 46526.

NREL prints on paper that contains recycled content.

Correlative nm-Scale Nonuniformity of Active Charge Carriers and Electrical Potential along both the Plane-View and Depth Directions in Group-V-Doped CdTe Thin Films

Chun-Sheng Jiang
National Renewable Energy Laboratory
Golden, USA
chun.sheng.jiang@nrel.gov

John Moseley
National Renewable Energy Laboratory
Golden, USA
john.moseley@nrel.gov

Chunxioao Xiao
National Renewable Energy Laboratory
Golden, USA
chuanxiao.xiao@nrel.gov

Wyatt Metzger
National Renewable Energy Laboratory
Golden, USA
wyatt.metzger@nrel.gov

Mowafak Al-Jassim
National Renewable Energy Laboratory
Golden, USA
mowafak.aljassim@nrel.gov

***Abstract*—We report nanometer-scale imaging on inhomogeneous distributions of active carrier and electrical potential in an As-doped CdTe film along both plane-view and film-depth directions. Despite Se grading, the scanning capacitance microscopy imaging does not show a clear variation of carrier concentration along the depth of the film. Instead, we observe carrier concentration variations of about 1 order of magnitude (high 10^{15} to low $10^{17}/cm^3$), with inhomogeneous spatial regions ranging from a few hundred nm to a few μm. This nonuniformity is distributed randomly in both the film lateral and vertical directions, independent of grain structure and grain boundaries (GBs). We further mapped the surface potential using Kelvin probe force microscopy. Higher potential was found on GBs, illustrating positive GB charging but not GB-specific carrier concentration. The results indicate that this suite of techniques can identify nonuniform carrier concentration and potential fluctuations that can contribute to open-circuit voltage deficits in group-V-doped CdTe devices.**

Keywords— CdTe thin-film photovoltaics, group-V doping, nonuniform doping concentration, nonuniform electrical potential, scanning capacitance microscopy, Kelvin probe force microscopy.

I. INTRODUCTION

State-of-the-art CdTe thin-film solar cells have made recent efficiency gains mainly by improving short-circuit current density [1] and the minority-carrier lifetime by alloying Se into the CdTe layer [2]. With photocurrent near its maximum, the limited Cu-doping on the order of $10^{14}/cm^3$ has become one focus for further improving open-circuit voltage (V_{oc}) [3], and there are significant efforts to increase carrier concentration by group-V doping [4][5][6][7][8][9]. Indeed, average carrier concentrations have been improved to $>10^{16}/cm^3$ as evidenced by capacitance-voltage (C-V) characterization [4][5]. Next steps are device integration and realizing potential voltage gains. A plausible cause for suboptimal voltage is nonuniform doping and resulting potential fluctuations [10]. Here, we indicate that *active-carrier* imaging with *nanometer resolution* can examine doping distribution to guide decreasing the V_{oc} deficit.

We have reported nm-scale imaging of active-carrier distribution of As-doped CdTe film by developing scanning capacitance microscopy (SCM) [11]. The state-of-the-art CdTe devices incorporate Se near the front junction, so the doping and active-carrier concentration can vary from the front to the back of the film. Here, we report SCM imaging on beveled samples to measure the carrier distribution through the depth of the film as well as laterally.

The SCM technique was established for crystalline Si (c-Si) carrier delineation by forming a high-quality thermal SiO_x layer on top of a Si sample, and it is widely used by the Si micro-device industry [12][13]. SCM is currently the most powerful imaging technique for *active-carrier* concentration with tens of nm resolution. Here, we apply SCM to CdTe and calibrate the SCM measurement for thin-film CdTe using measurements on a sample deposited by molecular beam epitaxy (MBE) in which the doping was varied at discrete stages [11]. We found that the carrier concentration in the As-doped CdTe film is randomly nonuniform along both the lateral and vertical directions, which can be one of the root causes for V_{oc} deficit. However, we did not observe a significant trend of systematic variation in carrier concentration along the depth of the film. We also imaged the electrical potential on the same sample area using Kelvin probe force microscopy (KPFM) [14][15] to cross-examine the potential fluctuation [11]. The results further provided nm-scale understanding about the electronic inhomogeneity of the films.

This report is available at no cost from the National Renewable Energy Laboratory at www.nrel.gov/publications.

II. Experiment

The As-doped CdTe film was grown by vapor-transport deposition (VTD). The SCM technique requires a metal/insulator/semiconductor (MIS) structure formed by the AFM metal probe (Rocky Mountain Nanotechnology LLC, 25Pt300B), an insulating layer, and the CdTe film. A high-quality insulating layer with minimium charges trapped in the layer and at the interface and a thin layer thickness (10–30 nm) are critical requirements for high-quality SCM imaging [12]. We have developed a procedure for the sample preparation by annealing it in a low-vacuum oven at 280ºC for 2 h, which grows a good insulating layer as evidenced by the SCM signal quality on a known MBE sample where doping was increased in staircase fashion throughout the film [11]. Before annealing the sample, we made micro-bevels with ~30º angles using focused ion-beam (FIB) milling (see Fig. 1). For KPFM, which also needs an anneal to passivate the film surface, the proper anealing is 250ºC for 5 min. The insulating layer nessessary for SCM conceals the CdTe surface-potential contrast for KPFM, so a lighter annealing for surface passivation is only proper for KPFM [11].

Our SCM and KPFM are based on the contact and non-contact modes of the atomic force microscope (AFM, Veeco D5000 and Nanoscope V). The SCM capacitance sensor is a RCA-type radio-frequency resonator (Veeco, SCM module) with a sensitivity of $\sim10^{-18}$ F, and the KPFM is custom-made using the second-harmonic oscillation of the cantilever with enhanced voltage sensitivity of ~10 mV.

III. Results and Discussions

We first discuss the SCM carrier distribution of the As-doped film, followed by a cross-examination of KPFM imaging on the same sample area.

SCM provides a relative concentration contrast of active carriers by detecting the local dC/dV signal of the MIS structure using a lock-in amplifier [12]. Qualitatively, a larger dC/dV signal indicates lower carrier concentration. Holes and electrons can be distinguished because they have opposite dC/dV signs. Although the direct output of the lock-in amplifier is in volts, it gives a relative scale of carrier concentration. To quantify the carrier concentration in an SCM image, the carrier concentration should be known in at least one point, then the concentration at other points can be deduced [12].

Figures 2a and 2b show SCM and corresponding AFM images taken on the beveled surface. Figure 2c and 2d show a dC/dV line profile along the lateral white dashed line in Fig. 2a and the converted carrier concentration, respectively. The line profile is along the depth direction and across the junction. The SCM dC/dV is negative at the transparent conductive oxide (TCO) and positive at the CdSeTe regions, showing n-type and p-type active carriers, respectively. We converted the SCM dC/dV measurement to carrier concentration using a simple one-dimensional approximation [11]. The MIS capacitance is the sum of two serially connected components of insulating-layer capacitance and underlying semiconductor space-charge-region capacitance. In the depletion region close to the p-n

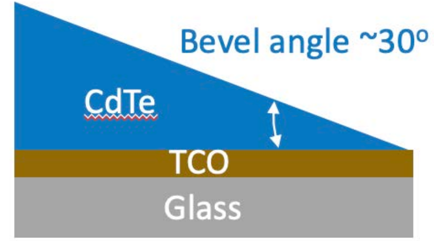

Fig. 1. A schematic showing the beveled sample preparation.

transition point with dC/dV=0, because an additional junction electric field is present, the 1D carrier conversion from the MIS capacitance cannot be applied; the carrier concentration is presented only in the region outside the depletion region (Fig. 2d). This 1D capacitance calculation can significantly deviate from the actual 3D measurement with a sharp probe size of ~20 nm; therefore, the carrier concentration is qualitative or semi-quantitative.

Figures 2e and 2f show the SCM dC/dV and carrier concentration along the vertical white line in Fig. 2a in the CdSeTe absorber outside the depletion regions. The carrier concentration as revealed by the image and profiles is nonuniform—with overall variation of more than one order of magnitude (high 10^{15}/cm^3 ~ low 10^{17}/cm^3), and with variation size from hundreds of nm to several μm. The amount of Se incorporated in CdTe has a gradient extending about 1 μm from the junction, with no significant alloying beyond 1 μm from the junction interface. The As doping and active-carrier concentrations can vary with Se alloying. However, the active-carrier imaging does not show a clear trend of variation along the film depth direction, and this was further illustrated by the depth profile averaged from the image (Fig. 3). The carrier concentration appears to be randomly distributed through the entire absorber. The carrier concentration is not correlated with grain boundaries (GBs), grain structure, grain orientation, film depth, or lateral features. The mechanism causing the "random" active-carrier concentration is not currently clear. The average active-carrier concentration of $\sim10^{16}$/cm^3 is much lower than the As-incorporation level of $\sim10^{18}$/cm^3. This low activation rate can be caused by defects such as AX-center or compensating defects [16][17]. The size and amplitudes of the nonuniformity should correlate to the interaction strength and range of the defects such as As_{Te}^{+} or As_{Se}^{+} acceptors and/or compensating defects. The low activation rate of several percent and carrier fluctuation suggest that further understanding and innovation/optimization of the Gr-V doping are needed [4].

This report is available at no cost from the National Renewable Energy Laboratory at www.nrel.gov/publications.

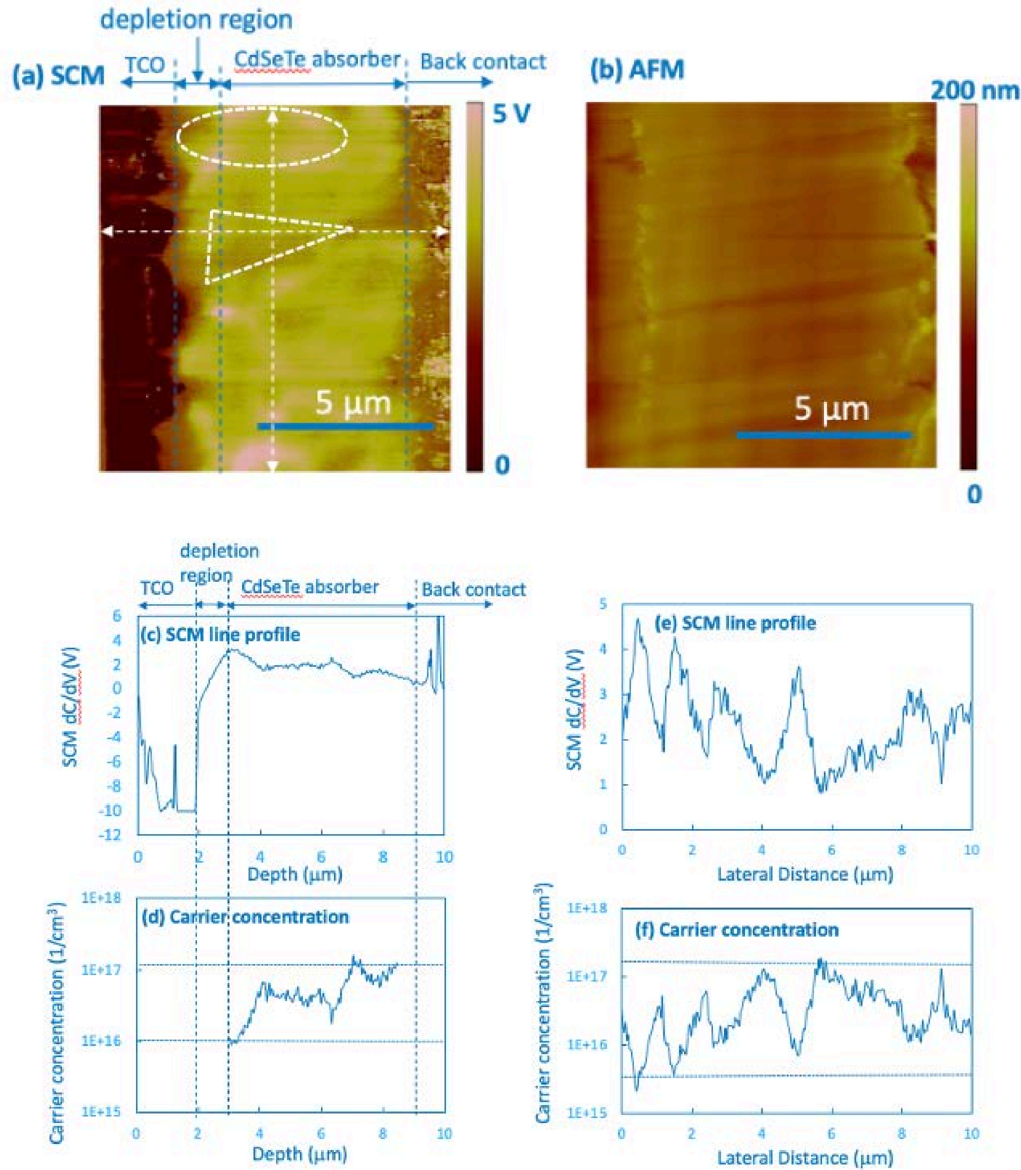

Fig. 2 (a) A SCM and (b) the corresponding AFM images taken on a beveled CdSeTe/CdTe device; (c) SCM and (d) semi-quantitively converted carrier-concentration line profiles along the lateral line in Fig. 2(a); (e) and (f) are profiles along the vertical white line. Dashed oval and triangle in (a) are for comparisons with features in Fig. 4(b).

We further imaged the electrical potential on the same beveled sample area using KPFM. Figures 4a and 4b show the KPFM raw data and the image after "flattening" to remove the background level that enhanced the potential contrast. Figure 4c shows a potential line profile along the lateral white line in Fig. 4a across the junction; and Figures 4d and 4e show the potential along the two vertical lines in Fig. 4b to exhibit the potential variations in regions near the junction and the back contact. The potential contrast across the junction is ~250 mV (Fig. 4c), which is smaller than the built-in potential in the device bulk; this is because the different surface charges or surface band bending reduce the potential contrast by opposite charges (negative or positive) on the surface of n- and p-type semiconductors [18][19]. The relative GB potential to the grain interior illustrates weakly charged GBs with 30–50-mV potential contrast near the junction (Fig. 4d). The contrast in the region near the back contact is 30–70 mV (Fig. 4e). Note that the surface-potential contrast measured by this technique may differ from that in the bulk [18][19].

This report is available at no cost from the National Renewable Energy Laboratory at www.nrel.gov/publications.

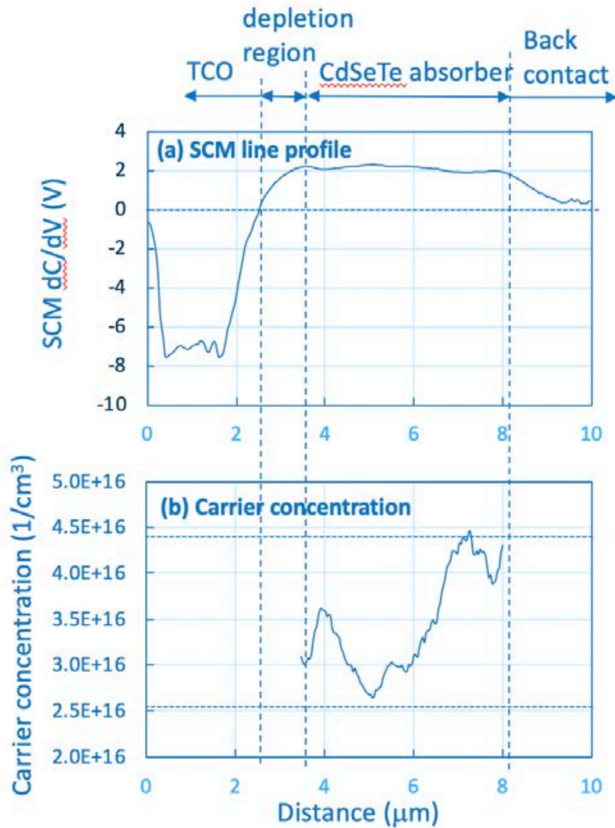

Fig. 3(a) SCM and 3(b) converted carrier concentration profiles averaged vertically from Fig. 2(a).

Close examination of Figs. 2 and 4 leads to two observations: 1) GBs are clear in the KPFM image but not in the SCM image, which illustrates that the GBs are positively charged but do not have different carrier concentrations from the grain interior; and 2) a vague agreement of the overall contrasts of SCM and KPFM can be observed. For example, a bright area in the SCM image (Fig. 2a) and KPFM image (Fig. 4b) are indicated by dashed ovals, and a dark area is indicated by dashed triangles. As discussed in the previous paper [11], the GB potential-induced carrier concentration depletion would be small below the SCM detection limit, which is different from the doping-induced potential variation with a large capacitance change that can be detected by SCM.

The vague agreement between the SCM and KPFM images can be qualitatively explained by considering that a higher dC/dV indicates a lower carrier concentration (Figs. 2c–2f), then a lower valence-band maximum (VBM) relative to the flat Fermi level or a larger energy interval in the electronic band diagram (the thermal-equilibrium state), and thus, a higher (positive) local potential. The one order-of-magnitude variation in carrier concentrations would correspond to a potential fluctuation of $\Delta E = kT\ln(10) \sim 60\ mV$ at room temperature T = 300 K, which is comparable to the overall KPFM potential fluctuation of 30–70 mV between regions of the absorber (without accounting for the potential contrast between GB and grain interior).

IV. Summary

We report nanometer-scale imaging of inhomogeneous active-carrier distribution of an As-doped CdTe film along both the plane-view and film-depth directions by measuring on a beveled sample geometry. Despite the Se-alloying grading along the depth direction, the SCM imaging does not show a corresponding variation of carrier concentration. Instead, we observed nonuniform concentrations with inhomogeneous sizes from sub-μm to a few μm, and concentration variation of more than one order of magnitude (high 10^{15} to low $10^{17}/cm^3$). This nonuniformity is distributed randomly in both the lateral and vertical directions and independent of grain structure and GBs. We further mapped the surface potential by KPFM. Higher potential was found on the GBs, whereas a corresponding contrast in carrier concentration was not found by SCM, illustrating positive GB charging but not GB-specific carrier concentration. The results indicate that this suite of techniques can identify nonuniform carrier concentration and potential fluctuations that can contribute to V_{oc} deficits in Group-V-doped CdTe devices.

Acknowledgment

This work was supported by the U.S. Department of Energy under Contract No. DE-AC36-08GO28308 with the Alliance for Sustainable Energy, LLC, the Manager and Operator of the National Renewable Energy Laboratory. Funding was provided by the U.S. Department of Energy Office of Energy Efficiency and Renewable Energy Solar Energy Technologies Office. The U.S. Government retains and the publisher, by accepting the article for publication, acknowledges that the U.S. Government retains a nonexclusive, paid-up, irrevocable, worldwide license to publish or reproduce the published form of this work, or allow others to do so, for U.S. Government purposes.

[1] M. A. Green *et al.*, "Solar cell efficiency tables (version 50)," *Progress in Photovoltaics: Research and Applications*, vol. 25, no. 7, pp. 668–676, 2017, doi: 10.1002/pip.2909.

[2] M. Gloeckler, I. Sankin, and Z. Zhao, "CdTe Solar Cells at the Threshold to 20% Efficiency," *IEEE Journal of Photovoltaics*, vol. 3, no. 4, pp. 1389–1393, Oct. 2013, doi: 10.1109/JPHOTOV.2013.2278661.

[3] A. Kanevce, M. O. Reese, T. M. Barnes, S. A. Jensen, and W. K. Metzger, "The roles of carrier concentration and interface, bulk, and grain-boundary recombination for 25% efficient CdTe solar cells," *Journal of Applied Physics*, vol. 121, no. 21, p. 214506, Jun. 2017, doi: 10.1063/1.4984320.

[4] W. K. Metzger *et al.*, "Exceeding 20% efficiency with in situ group V doping in polycrystalline CdTe solar cells," *Nature Energy*, vol. 4, no. 10, pp. 837–845, Oct. 2019, doi: 10.1038/s41560-019-0446-7.

This report is available at no cost from the National Renewable Energy Laboratory at www.nrel.gov/publications.

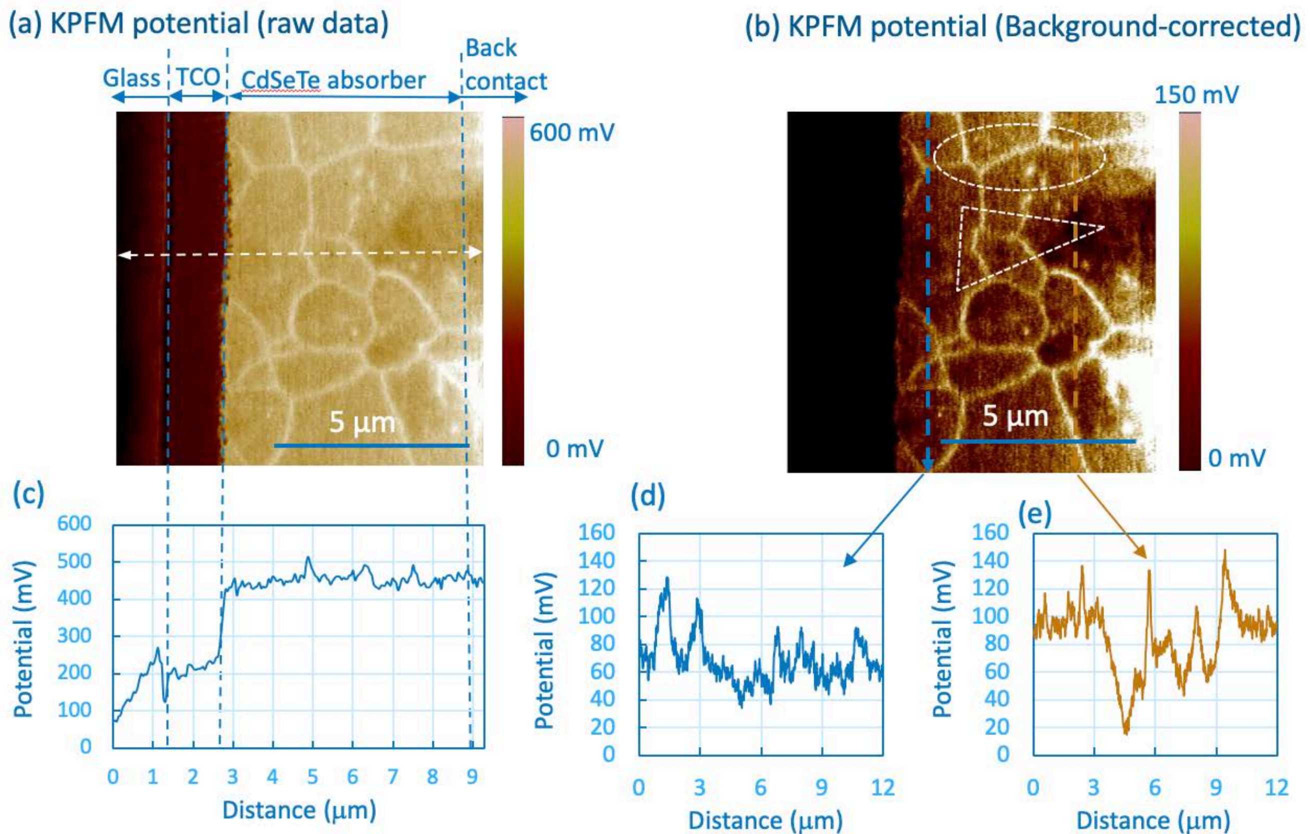

Fig. 4(a) A KPFM and 4(b) flattened KPFM images taken on the same area as Fig. 2(a); (c)–(e) show potential line profiles along the white lines in Fig. 4(a) and blue and orange lines in 4(b). Dashed oval and triangles are for comparisons with features in Fig. 2(a).

[5] J. M. Burst *et al.*, "CdTe solar cells with open-circuit voltage breaking the 1 V barrier," *Nature Energy*, vol. 1, no. 3, pp. 1–8, Feb. 2016, doi: 10.1038/nenergy.2016.15.
[6] E. Colegrove *et al.*, "Phosphorus Diffusion Mechanisms and Deep Incorporation in Polycrystalline and Single-Crystalline CdTe," *Phys. Rev. Applied*, vol. 5, no. 5, p. 054014, May 2016, doi: 10.1103/PhysRevApplied.5.054014.
[7] J. N. Duenow *et al.*, "Relationship of Open-Circuit Voltage to CdTe Hole Concentration and Lifetime," *IEEE Journal of Photovoltaics*, vol. 6, no. 6, pp. 1641–1644, Nov. 2016, doi: 10.1109/JPHOTOV.2016.2598260.
[8] B. E. McCandless *et al.*, "Overcoming Carrier Concentration Limits in Polycrystalline CdTe Thin Films with In Situ Doping," *Scientific Reports*, vol. 8, no. 1, p. 14519, Sep. 2018, doi: 10.1038/s41598-018-32746-y.
[9] A. Nagaoka *et al.*, "Comparison of Sb, As, and P doping in Cd-rich CdTe single crystals: Doping properties, persistent photoconductivity, and long-term stability," *Appl. Phys. Lett.*, vol. 116, no. 13, p. 132102, Mar. 2020, doi: 10.1063/5.0004883.
[10] U. Rau and J. H. Werner, "Radiative efficiency limits of solar cells with lateral band-gap fluctuations," *Appl. Phys. Lett.*, vol. 84, no. 19, pp. 3735–3737, Apr. 2004, doi: 10.1063/1.1737071.
[11] C.-S. Jiang *et al.*, "Imaging hole-density inhomogeneity in arsenic-doped CdTe thin films by scanning capacitance microscopy," *Solar Energy Materials and Solar Cells*, vol. 209, p. 110468, Jun. 2020, doi: 10.1016/j.solmat.2020.110468.
[12] C. C. Williams, "Two-Dimensional Dopant Profiling by Scanning Capacitance Microscopy," *Annual Review of Materials Science*, vol. 29, no. 1, pp. 471–504, 1999, doi: 10.1146/annurev.matsci.29.1.471.
[13] C.-S. Jiang *et al.*, "Imaging charge carriers in potential-induced degradation defects of c-Si solar cells by scanning capacitance microscopy," *Solar Energy*, vol. 162, pp. 330–335, Mar. 2018, doi: 10.1016/j.solener.2017.12.025.
[14] M. Nonnenmacher, M. P. O'Boyle, and H. K. Wickramasinghe, "Kelvin probe force microscopy," *Appl. Phys. Lett.*, vol. APLCLASS2019, no. 1, pp. 2921–2923, Jun. 1998, doi: 10.1063/1.105227@apl.2019.APLCLASS2019.issue-1.
[15] A. Kikukawa, S. Hosaka, and R. Imura, "Silicon pn junction imaging and characterizations using sensitivity enhanced Kelvin probe force microscopy," *Appl. Phys. Lett.*, vol. 66, no. 25, pp. 3510–3512, Jun. 1995, doi: 10.1063/1.113780.
[16] T. Ablekim *et al.*, "Self-compensation in arsenic doping of CdTe," *Scientific Reports*, vol. 7, no. 1, p. 4563, Jul. 2017, doi: 10.1038/s41598-017-04719-0.
[17] S.-H. Wei and S. B. Zhang, "Chemical trends of defect formation and doping limit in II-VI semiconductors: The case of CdTe," *Phys. Rev. B*, vol. 66, no. 15, p. 155211, Oct. 2002, doi: 10.1103/PhysRevB.66.155211.
[18] C.-S. Jiang *et al.*, "Local built-in potential on grain boundary of Cu(In,Ga)Se2 thin films," *Appl. Phys. Lett.*, vol. 84, no. 18, pp. 3477–3479, Apr. 2004, doi: 10.1063/1.1737796.
[19] C.-S. Jiang *et al.*, "Nanometer-scale surface potential and resistance mapping of wide-bandgap Cu(In,Ga)Se2 thin films," *Appl. Phys. Lett.*, vol. 106, no. 4, p. 043901, Jan. 2015, doi: 10.1063/1.4907165.

This report is available at no cost from the National Renewable Energy Laboratory at www.nrel.gov/publications.